

## Influence of the Electron-Cation Interaction on Electron Mobility in Dye-Sensitized ZnO and TiO<sub>2</sub> Nanocrystals: A Study Using Ultrafast Terahertz Spectroscopy

H. Němec,<sup>1,3</sup> J. Rochford,<sup>2</sup> O. Taratula,<sup>2</sup> E. Galoppini,<sup>2</sup> P. Kužel,<sup>3</sup> T. Polívka,<sup>4</sup>  
A. Yartsev,<sup>1</sup> and V. Sundström<sup>1</sup>

<sup>1</sup>*Department of Chemical Physics, Lund University, Getingevägen 60, Box 124, 221 00 Lund, Sweden*

<sup>2</sup>*Chemistry Department, Rutgers University, 73 Warren Street, Newark, New Jersey 07102, USA*

<sup>3</sup>*Institute of Physics of the Academy of Sciences of the Czech Republic, Na Slovance 2, 182 21 Praha 8, Czech Republic*

<sup>4</sup>*Institute of Physical Biology, University of South Bohemia, Zámek 136, CZ-373 33 Nové Hradky, Czech Republic*

(Received 18 August 2009; published 13 May 2010)

Charge transport and recombination in nanostructured semiconductors are poorly understood key processes in dye-sensitized solar cells. We have employed time-resolved spectroscopies in the terahertz and visible spectral regions supplemented with Monte Carlo simulations to obtain unique information on these processes. Our results show that charge transport in the active solar cell material can be very different from that in nonsensitized semiconductors, due to strong electrostatic interaction between injected electrons and dye cations at the surface of the semiconductor nanoparticle. For ZnO, this leads to formation of an electron-cation complex which causes fast charge recombination and dramatically decreases the electron mobility even after the dissociation of the complex. Sensitized TiO<sub>2</sub> does not suffer from this problem due to its high permittivity efficiently screening the charges.

DOI: 10.1103/PhysRevLett.104.197401

PACS numbers: 78.67.Bf, 72.20.-i, 73.23.-b, 78.47.J-

Nanostructured materials for, e.g., photovoltaics, catalysis, sensors, light emitting devices, etc., rely on charge transport that occurs on a wide distribution of time and distance scales. The ultrafast time scale associated with transport within and between individual nanostructural components is poorly understood and cannot be addressed by electrical techniques.

The operation of a dye-sensitized solar cell relies on the efficient electron injection from a photoexcited sensitizer molecule to the conduction band of a semiconductor, leading to the formation of mobile electrons (and a dye cation). The generally accepted picture is that mobile electrons appear in concert with injection. Our results show that charge injection and formation of mobile charges are not necessarily connected, and that charge transport in the sensitized solar cell material can differ from that in bulk or nanocrystalline nonsensitized semiconductors. This is related to strong electrostatic interaction between injected electrons and dye cations at the surface of the semiconductor nanoparticle (NP).

In this Letter, we investigate ultrafast dynamics in ZnO and TiO<sub>2</sub> NPs (mean diameters 15 and 9 nm, respectively) sensitized by Zn(II)-5-(3,5-dicarboxyphenyl)phenyl-10,15,20-triphenylporphyrin (ZnTPP-Ipa) and Ru(2,2'-bipyridyl-4,4'-dicarboxylic acid)<sub>2</sub>(NCS)<sub>2</sub> · 2H<sub>2</sub>O (Ru-N3) dyes [1,2]. A concerted use of THz spectroscopy, optical transient absorption (TA) spectroscopy, and Monte Carlo simulations allows us to obtain a microscopic picture of electron injection and transport in nanostructured dye-sensitized semiconductors, the active part in a Grätzel type of solar cell [3].

Probing in the visible range provides information about the electronic state of the dye molecules and about the

formation of oxidized dye molecule (cation) upon electron injection [4–9]. The time-resolved THz spectroscopy provides contact-free access to the transient conductivity on subpicosecond to nanosecond time scales [10]. With this frequency range and time resolution the measured transient spectra directly reflect the charge motion on the scale of the size of nanostructural components and contain fingerprints of both intra- and interparticle transport mechanisms [11,12]. Although a few reports on measurement of transient THz conductivity in bare and sensitized TiO<sub>2</sub> and ZnO NPs were published [13–15], a comprehensive picture of the ultrafast charge transport has not been established yet.

The transient THz conductivity as a function of time  $\tau_p$  after photoexcitation was measured in a usual setup for optical pump–THz probe experiments based on a Ti:sapphire femtosecond laser amplifier [12]. The samples were excited either in UV to photogenerate electrons in the semiconductor through interband photoexcitation, or in the visible, which leads to injection of electrons from the dye into the semiconductor. For the observed slow dynamics, the transient effective conductivity of the sample  $\Delta\sigma_{\text{eff}}(f, \tau_p)$  is proportional to the ratio of the transient THz spectrum  $\Delta E(f, \tau_p)$  transmitted through the excited sample and a reference THz spectrum  $E_0(f)$  acquired with pump beam off [12]. The influence of inhomogeneity of the films was accounted for by effective medium approximation. For the studied systems, the intrinsic conductivity  $\Delta\sigma$  of carriers in NPs is linearly proportional to the measured (effective) conductivity  $\Delta\sigma_{\text{eff}}$  [11]. Note that the intrinsic conductivity  $\Delta\sigma$  normalized by the excitation density  $\Delta n_{\text{exc}}$  and by the elementary charge [ $\Delta\sigma/(\Delta n_{\text{exc}}e_0)$ ] is the key quantity measured by time-resolved THz spectroscopy.

copy: it is a product of the fraction of mobile charge carriers and of their mobility  $\mu$ . TA experiments were performed using a standard TA spectrometer based on a 1 kHz laser amplifier [16]. The pump pulse was polarized at the magic angle to the polarization of the white-light-continuum probe.

THz kinetics reflects the population of mobile electrons in the semiconductor. In Fig. 1(a) we see that after dye excitation of both ZnTPP-Ipa/ZnO and Ru-N3/ZnO, the rise of the population of injected mobile electrons occurs on the tens to hundreds-ps time scale. The corresponding rise for ZnTPP-Ipa/TiO<sub>2</sub> and Ru-N3/TiO<sub>2</sub> occurs on the sub-ps and few ps time scale. This shows that the slow appearance of mobile electrons is related to a property of ZnO NPs. Mid-IR probe of injection of conduction band electrons in RuN3/ZnO has previously demonstrated a similar slow kinetics [4,6]. This shows that both THz and mid-IR radiation probe mobile electrons.

The conventional picture of electron injection is that mobile electrons appear in concert with oxidized dye. This concept can now be tested by comparison of visible TA dynamics, which probe the appearance of oxidized dye, with the THz dynamics. Figure 1(b) shows that for ZnTPP-Ipa/ZnO the formation of a species (rise of TA

kinetics, see Ref. [2] for details) with a cationlike spectrum is completed within  $\sim 5$  ps. In the experiments of Katoh *et al.* on Ru-N3/ZnO [6,17] a species with spectral characteristics similar to that of the Ru-N3 cation (termed exciplex) was observed immediately after excitation ( $\sim 100$  fs). Thus, for ZnO sensitized with both ZnTPP-Ipa and Ru-N3 the formation of a species with spectral properties similar to those of the oxidized dye is very fast ( $< 5$  ps) and precedes the much slower formation of mobile electrons on the tens and hundreds of ps time scale. This behavior can be understood within the kinetic scheme of Fig. 1(c), involving an intermediate state between the excited state of the sensitizer ( $D^*$ ) and the cation with mobile electrons in the conduction band of ZnO ( $D^+ + e^-_{\text{mobile}}$ ). Thus, photoexcitation of the sensitizer (1) leads to an electron-cation (EC) complex within  $\sim 5$  ps (3) in which the electron is strongly bound to the cation and therefore it does not contribute to the THz signal, whereas the TA spectrum of the EC complex is similar to that of the cation (Fig. A2 in Ref. [2]). This bound EC state can either recombine (5) or dissociate into a mobile electron in ZnO and cation (4). The existence of the EC state is further confirmed by a global fit of TA spectra [2].

The initial part of the TA decay of ZnTPP-Ipa/ZnO [Fig. 1(b)] reflects the depopulation of the EC complex caused by recombination (5) (approximately 75%) and cation formation (4) (approximately 25%) [2]. Because of the very slow recombination of injected electrons (6), the THz signal at long times ( $\geq 1$  ns) reflects the total population of injected mobile electrons, which is equal to the population of cations. From the scheme in Fig. 1(c) it can be predicted that the measured formation rate of mobile electrons should be equal to the observed decay rate of the EC complex through pathways (4) and (5) [2]. This is indeed confirmed by the perfect match of the rise of the THz kinetics and the decay of TA kinetics [see Fig. 1(b) where the two kinetics are superimposed]. Since there is no significant THz signal immediately after photoexcitation, we conclude that there is no substantial amount of mobile electrons injected into ZnO directly [(2) in Fig. 1(c)].

Since the observed intermediate state for ZnTPP-Ipa/ZnO has a clear cation signature from the TA spectra (see Fig. A2 in Ref. [2]) we prefer to refer to it as an EC complex. Note that the recombination (5) of the EC complex limits the number of mobile electrons injected into the conduction band of the semiconductor. We thus conclude that the EC complex recombination may decrease the efficiency of ZnO-based solar cells.

The presented view receives strong support from the injection-recombination dynamics observed for sensitized nanocrystalline TiO<sub>2</sub> films. The THz and TA kinetics of both dyes [Figs. 1(a) and 1(d) and Refs. [4–9]] show that both cations and mobile electrons appear on the same ultrafast time scale (100 fs–10 ps). This suggests that charge injection into TiO<sub>2</sub> is a direct process [(2) in Fig. 1(c)]. Slow electron-cation recombination (6) occur-

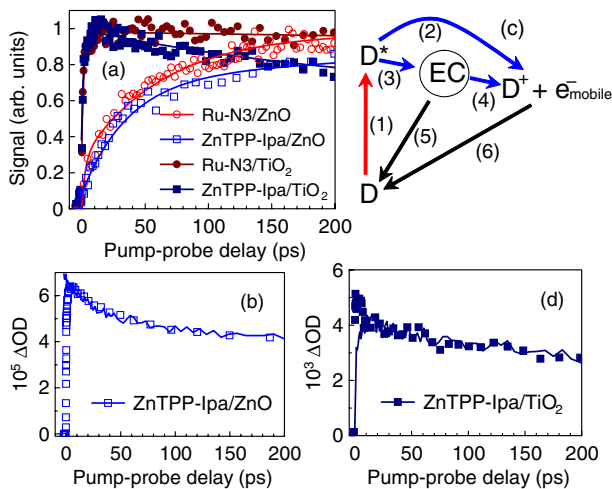


FIG. 1 (color online). (a) Evolution of transient THz conductivity (normalized to unity). The lines serve only to guide the eye. (b) Transient absorption of ZnTPP-Ipa/ZnO probed at 655 nm (symbols). This wavelength was selected due to the largest difference between the transient absorption of the initially excited state  $D^*$  and of the excitation products. The line represents a vertically flipped and shifted transient THz conductivity of ZnTPP-Ipa/ZnO from (a). Ru-N3 was excited at 400 nm; ZnTPP-Ipa was excited at 558 nm. (c) Scheme of the processes in dye-sensitized semiconductors. (1) Dye excitation, (2) direct electron injection, (3) formation of an electron-cation (EC) complex, (4) dissociation of EC complex, (5) recombination of EC complex and (6) charge recombination.  $D$ —dye molecule. (d) Transient absorption of ZnTPP-Ipa/TiO<sub>2</sub> probed at 655 nm (symbols). The line represents a shifted and scaled transient THz conductivity of ZnTPP-Ipa/TiO<sub>2</sub> from (a). Note that the line is not flipped, unlike in panel (b).

ring on a  $>100$  ps time scale is observed in ZnTPP-Ipa/TiO<sub>2</sub> as the decays in the TA and THz signals [Figs. 1(a) and 1(d)]. The common origin of these processes is underlined by the same decay rates [Fig. 1(d)]. The THz conductivity for Ru-N3/TiO<sub>2</sub> does not start to decay even on the nanosecond scale. Solar cells based on Ru-N3/TiO<sub>2</sub> can have a conversion efficiency of  $\sim 10\%$ . The somewhat faster electron-cation recombination in ZnTPP-Ipa/TiO<sub>2</sub> may contribute to a lower solar cell efficiency of 4%–5% for similar porphyrin sensitizers [18].

Transient far-infrared conductivity spectra (Fig. 2) provide information on the local transport of carriers photogenerated in the semiconductor or injected into the semiconductor. The observed spectra of photogenerated carriers in bare semiconductors do not exhibit the typical Drude response of free carriers in bulk, but the response can be accounted for if electrons move freely inside the NPs, whereas electron transport between neighboring particles is rare. This was discussed in detail in Ref. [11]: Monte Carlo simulations of charge carrier motion showed that our spectra can be explained assuming that the probability that an electron is transported from one NP to another upon reaching its surface is 10% and 5% in ZnO and TiO<sub>2</sub> NPs, respectively. The difference between the spectra of ZnO and TiO<sub>2</sub> are mainly related to the large difference in effective electron masses. The shape of the conductivity spectrum (i.e., namely, the ratio between the real and imaginary part) is the same for carriers photogenerated in bare and sensitized NPs [19]. This means that attachment of neutral dye molecules does not influence the electron transport properties.

Apart from the amplitudes which are related to the charge yield, the conductivity spectra of electrons injected into TiO<sub>2</sub> NPs from either Ru-N3 or ZnTPP-Ipa are the

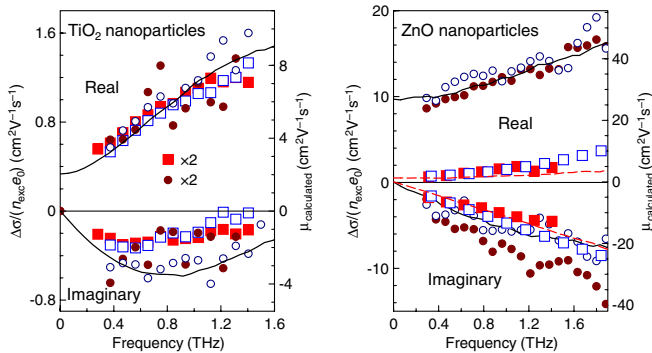
same as the spectrum of photogenerated electrons in TiO<sub>2</sub> [19]. We thus conclude that dye molecules either in their neutral or oxidized state do not influence transport of electrons in TiO<sub>2</sub>.

In contrast, the conductivity spectrum of injected electrons in ZnO differs from the spectrum of photogenerated electrons; namely, the real part of conductivity is considerably lower. Our hypothesis is that cations restrict the motion of injected electrons even after these escape from the EC complex. The interaction between the cations and the injected electrons is necessarily electrostatic. This interaction is screened in TiO<sub>2</sub> NPs due to their high permittivity (80 compared to 8 in ZnO) so that the oxidized dye molecules do not influence electron transport in TiO<sub>2</sub>, in agreement with our observations.

In order to confirm our hypothesis and to further understand the influence of dye cations on the electron transport in ZnO, we investigated the response of electrons localized within the NPs and moving in a model potential. The electron mobility was calculated using a Monte Carlo method [11]. For the sake of simplicity, we consider that the semiconductor NPs are nanocubes. Following Ref. [11] we consider that the surface reflects electrons with probability  $p_r = 0.8$  and scatters them in a random direction with probability  $1 - p_r$ . We used a harmonic potential within a pair of NPs with a minimum located at the NP surface expressing the attractive electrostatic force [Fig. 3(a)]. The repulsive force which prevents recombination in the real system is mimicked by the low permeability of the NP interface (high  $p_r$ ). In the experiment, we have on average 1.6 excited dye molecules per NP and the sketched potential profile correctly reflects even the cation density. Under these conditions, the calculations match the experimental data for a harmonic potential with the eigenfrequency of 10 THz. Though this model is very approximate, it provides the basic idea of the potential barrier for the electron transport which is about 100 meV [see Fig. 3(a)]. The electron localization caused by the potential is illustrated by the electron distribution function plot in Fig. 3(b).

There is a large number of theoretical and experimental works on electron transport in dye-sensitized semiconductors [20–24]. Most of these works focused on time scales much longer than those dealt with in this Letter. The assumptions of our model of transient conductivity closely resemble those of the “random flight model” [21]. We observe the “flight” phase of this model: the electron trapping occurs mainly at longer times (a characteristic capture time deduced from pump-probe scans in bare ZnO NPs is  $\sim 400$  ps). Note that the present measurements emphasize the importance of the NP connectivity which has been investigated by Cass *et al.* [25]. Similar quantities were accessed by transient conductivity measurements at 9 GHz [26], where the transport over several NPs was probed; consequently, an order of magnitude lower mobility was found than at THz frequencies.

In summary, we have investigated the dynamics and transport properties of electrons in nanostructured semi-



	Direct generation		Injection	
	—	ZnTPP-Ipa	Ru-N3	ZnTPP-Ipa
Sensitizer	—	ZnTPP-Ipa	Ru-N3	ZnTPP-Ipa
Symbol	●	○	□	■
Wavelength (nm)	300 (TiO <sub>2</sub> ) or 266 (ZnO)		400	558
Fluence (10 <sup>14</sup> ph/cm <sup>2</sup> )	1 (TiO <sub>2</sub> ) or 0.7 (ZnO)		4	2
Pump-probe delay (ps)	20		300	

FIG. 2 (color online). Summary of transient far-infrared conductivity spectra in various samples. Symbols (left axis): measured data; lines (right axis): calculated mobility of directly photogenerated electrons (solid) and injected electrons (dashed). These lines overlap in the left graph.

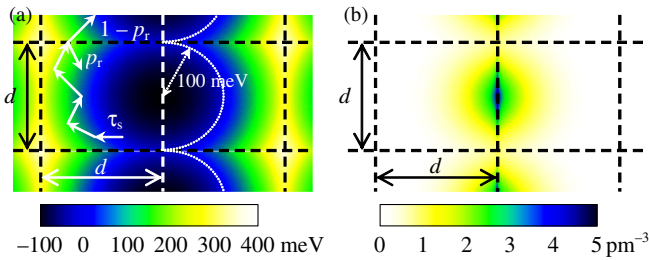


FIG. 3 (color online). (a) Geometry employed in the Monte Carlo simulations. Electrons interact with NP surfaces (dashed lines) and their momentum is randomly scattered with the mean time  $\tau_s$ . The color scale indicates the potential energy profile. (b) Electrons distribution in the semiconductor NPs.

conductors, generated by injection from excited sensitizers or direct excitation of the semiconductor. Electron injection into ZnO results in the formation of a bound electron-cation complex, which breaks up into an electron and cation or recombines on the time scale of tens to hundreds of picoseconds. The mobility of electrons that escape from the complex is strongly impaired by attractive electrostatic interaction with the cation at the semiconductor surface. In TiO<sub>2</sub>, injection results in instantaneous formation of mobile electrons and the charge recombination is very slow. We attribute the different charge transport and recombination in the two semiconductors to the screening of the electrostatic interaction in TiO<sub>2</sub> due to its high dielectric permittivity. Direct photoexcitation of the semiconductor results in instantaneous formation of mobile electrons for both ZnO and TiO<sub>2</sub>. Electrons also jump between particles with low probability. The combination of THz and visible TA spectroscopy, enabling simultaneous detection of mobile electrons and oxidized sensitizer, was key for obtaining the presented picture.

ZnO is being explored as a promising material for many optoelectronics applications, including dye-sensitized solar cells, due to its ability to self-assemble into various nanostructures and its high intrinsic electron mobility [27]. The EC complex formation in dye-sensitized materials, with its consequences of fast charge recombination and drastically reduced mobility, could limit the use of ZnO as a solar cell material. On the other hand, these drawbacks can be possibly remedied by an improved technology of preparation, e.g., by coating the ZnO NPs with a thin layer of a high dielectric permittivity material.

We acknowledge P. Persson for fruitful discussions, T. Pascher for assistance with data analysis, and J.-B. Hamard for assistance with experiments. This work was supported by the Swedish Energy Agency, Swedish Institute, the K&A Wallenberg Foundation, the U.S. Department of Energy (DE-FG02-01ER15256), Rutgers Research

Council, Czech Science Foundation (202/09/P099), Academy of Sciences of the Czech Republic (A100100902), and Ministry of Education of the Czech Republic (LC-512).

- [1] J. Rochford and E. Galoppini, *Langmuir* **24**, 5366 (2008).
- [2] See supplementary material at <http://link.aps.org/supplemental/10.1103/PhysRevLett.104.197401> for sample preparation procedure and for details on interpretation of transient absorption kinetics.
- [3] M. Grätzel, *J. Photochem. Photobiol.*, **A 164**, 3 (2004).
- [4] R. Katoh *et al.*, *Coord. Chem. Rev.* **248**, 1195 (2004).
- [5] N. A. Anderson and T. Lian, *Annu. Rev. Phys. Chem.* **56**, 491 (2005).
- [6] J. B. Asbury *et al.*, *J. Phys. Chem. B* **105**, 4545 (2001).
- [7] G. Benkő *et al.*, *J. Am. Chem. Soc.* **124**, 489 (2002).
- [8] G. Benkő *et al.*, *J. Am. Chem. Soc.* **125**, 1118 (2003).
- [9] G. Benkő *et al.*, *J. Phys. Chem. B* **108**, 2862 (2004).
- [10] F. A. Hegmann, O. Ostroverkhova, and D. G. Cooke, *Photophysics of Molecular Materials* (Wiley-VCH Verlag GmbH & Co. KGaA, Weinheim, 2006), Chap. 7, pp. 367–428.
- [11] H. Němec, P. Kužel, and V. Sundström, *Phys. Rev. B* **79**, 115309 (2009).
- [12] L. Fekete *et al.*, *Phys. Rev. B* **79**, 115306 (2009).
- [13] E. Hendry *et al.*, *Nano Lett.* **6**, 755 (2006).
- [14] G. M. Turner, M. C. Beard, and C. A. Schmuttenmaer, *J. Phys. Chem. B* **106**, 11 716 (2002).
- [15] J. B. Baxter and C. A. Schmuttenmaer, *J. Phys. Chem. B* **110**, 25 229 (2006).
- [16] K. G. Jespersen *et al.*, *Org. Electron.* **7**, 235 (2006).
- [17] A. Furube *et al.*, *J. Phys. Chem. B* **107**, 4162 (2003).
- [18] H. Imahory and T. Umeyama, *J. Phys. Chem. C* **113**, 9029 (2009).
- [19] Amplitudes of THz conductivities measured in bare and sensitized TiO<sub>2</sub> NPs are certainly scaled by charge yields. However, their absolute values should be considered with care: (i) they may be affected by inhomogeneities of the samples and (ii) we observed a progressive bleaching of the excited volume in the sensitized TiO<sub>2</sub> films which was correlated with an amplitude decrease (the damage did not alter the shape of the transient conductivity spectrum).
- [20] J. Nelson and R. E. Chandler, *Coord. Chem. Rev.* **248**, 1181 (2004).
- [21] A. V. Barzykin and M. Tachiya, *J. Phys. Chem. B* **106**, 4356 (2002).
- [22] A. J. Frank, N. Kopidakis, and J. van de Lagemaat, *Coord. Chem. Rev.* **248**, 1165 (2004).
- [23] J. Bisquert, *Phys. Chem. Chem. Phys.* **10**, 3175 (2008).
- [24] M. Wang *et al.*, *Chem. Phys. Chem.* **10**, 290 (2009).
- [25] M. J. Cass *et al.*, *J. Phys. Chem. B* **107**, 113 (2003).
- [26] J. E. Kroeze, T. J. Savenije, and J. M. Warman, *J. Am. Chem. Soc.* **126**, 7608 (2004).
- [27] C. Klingshirm, *Chem. Phys. Chem.* **8**, 782 (2007).